Phase stability and electronic structure of $ScAl_3$ and $ZrAl_3$ and of Sc-stabilized cubic $ZrAl_3$ precipitates

J.-H. Xu
Department of Physics and Astronomy, Northwestern University, Evanston, Illinois 60208-3112 and Shanghai Institute of Metallurgy, Academy of Sciences of China, Shanghai 200 050, China

A. J. Freeman
Department of Physics and Astronomy, Northwestern University, Evanston, Illinois 60208-3112
(Received 18 September 1989; revised manuscript received 12 March 1990)

The structural stability and the electronic structure of $ScAl_3$ were studied using an all-electron, total-energy, local-density approach. The calculated results show that $ScAl_3$ in the $L1_2$ structure is energetically favored compared with the $D0_{22}$ structure by about 0.42 eV per formula unit. The calculated lattice constant (4.055 Å) is in fairly good agreement with experiment (4.10 Å). As a comparison, the calculated electronic and cohesive properties for $ZrAl_3$ in its metastable $L1_2$ and $D0_{22}$ phases are also presented. It is argued, on the basis of density-of-states results, that a cubic $Zr_{1-x}Sc_xAl_3$ compound (and also $Ti_{1-x}Sc_xAl_3$) might be a good candidate as a dispersed phase in the aluminum alloys for elevated temperature applications. To test this prediction, we determined the electronic structure and the stability of Sc-stabilized cubic $(Zr_{0.5}Sc_{0.5})Al_3$ using the same total-energy approach. The calculated total energy for $(Zr_{0.5}Sc_{0.5})Al_3$, which is about 0.24 eV per unit cell lower than the sum of the total energies of $ZrAl_3$ and $ScAl_3$, clearly indicates that cubic $(Zr_{0.5}Sc_{0.5})Al_3$ is energetically favored compared with a mixture of its constituents. Finally, an analysis of the results indicates that the stability of the aluminides appears to be understood in the rigid-band sense in terms of the band filling of the bonding states.

I. INTRODUCTION

A study of the early-transition-metal elements and the aluminum-rich compounds MAl_3 (M = Sc, Ti, V, Zr ,...) has twofold significance. First of all, it is interesting to note that in the observed variation of crystal structures across each early-transition-metal series[1,2] (cf. Table I), most of the MAl_3 compounds crystallize in the tetragonal $D0_{22}$ (or $TiAl_3$-type) structure (such as $TiAl_3$, VAl_3, $NbAl_3$, $TaAl_3$, and the high-temperature phase of $HfAl_3$), and fewer in the tetragonal $D0_{23}$ (or $ZrAl_3$-type) phase (such as $ZrAl_3$ and $HfAl_3$ in its low-temperature phase) or in the hexagonal $D0_{19}$ (or Ni_3Sn-type) structure (such as the low-temperature phase of YAl_3 and $LaAl_3$). $ZrAl_3$ has the cubic $L1_2$ (or Cu_3Au-type) structure as a metastable state,[3] and YAl_3 has been observed to have an $L1_2$ structure above 950 °C.[2] Only $ScAl_3$ was reported in an early study[4] to have the cubic $L1_2$ structure with a lattice constant of 4.10 Å at room temperature; an $L1_2$ structure was also reported recently[5] for $ScAl_3$, but no lattice constant was given. Note that except for a slight distortion along the c axis in both the $D0_{22}$ and $D0_{23}$ structures, all three structures ($L1_2$, $D0_{22}$, and $D0_{23}$) are fcc-derived structures (cf. Fig. 1), and all four ($L1_2$, $D0_{19}$, $D0_{22}$, and $D0_{23}$) are closed-packed structures. Therefore, to understand the force driving the atomic ordering one must investigate in detail the competition between the structural stability of the different crystal structures.

The second motivation for the present study is the need to find good finely dispersed and thermally stable phase particles for developing high-temperature aluminum alloys, e.g., the so-called super "alumalloy."[6] The fact that the $ZrAl_3$ cubic $L1_2$ phase is partially coherent with the aluminum matrix (the lattice mismatch between the cubic metastable phase and aluminum matrix is only about 1%) and that $ZrAl_3$ has a limited solubility in Al, lead Fine *et al.*[7] to suggest $ZrAl_3$ as a dispersoid phase in the Al-

TABLE I. Observed variation of the crystal structure in transition-metal trialuminides across the early-transition-metal series. HT and RT denote the high-temperature phase and room-temperature phase, respectively.

IIIB	IVB	VB
$ScAl_3$ ($L1_2$)	$TiAl_3$ ($D0_{22}$)	VAL_3 ($D0_{22}$)
$YA1_3$ ($L1_2$ above 950 °C) ($BaPb_3$[a] above 640 °C) ($D0_{19}$ RT)	$ZrAl_3$ ($D0_{23}$, $L1_2$)	$NbAl_3$ ($D0_{22}$)
$LaAl_3$ ($D0_{19}$)	$HfAl_3$ ($D0_{22}$ HT) ($D0_{23}$ RT)	$TaAl_3$ ($D0_{22}$)

[a] The rhombohedral $BaPb_3$ structure is a transitional structure between the stacking of the $D0_{19}$ and the stacking of the cubic $L1_2$ structures.

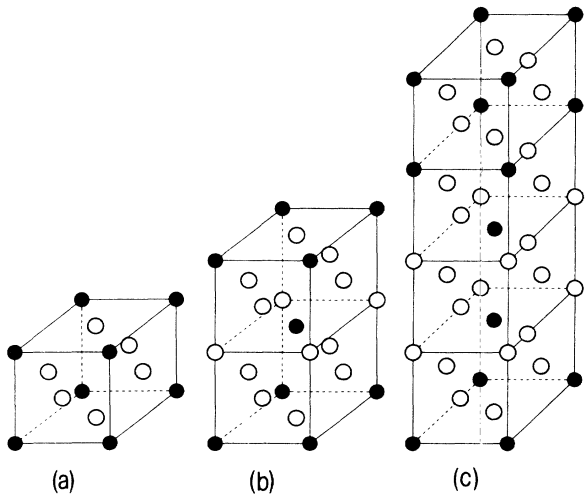

FIG. 1. Crystal structures for transition-metal trialuminides (a) $L1_2$, (b) $D0_{22}$, and (c) $D0_{23}$.

based alloys and to study[8] alloying in the Al-Ti, V, Zr, and Hf systems in order to further reduce the degree of lattice mismatch and to stabilize the cubic metastable $L1_2$ phase. Further, Chen *et al.*[9] found a low mismatch (hence, a low interfacial energy between the precipitates and the matrix) coherent coplanar $L1_2$ structured $Al_3(Zr_{0.25}V_{0.75})$ precipitates, which can retard the coarsening rate significantly. Clearly, from what was said earlier, since among the early-transition-metal trialuminides both $ScAl_3$ and $ZrAl_3$ (in its metastable phase) have (i) cubic $L1_2$ structure, (ii) close similarity between the lattice constants of $ScAl_3$ (or $ZrAl_3$) and the Al matrix, and (iii) high melting points and limited solubility in the Al matrix, both $ScAl_3$ and $ZrAl_3$ appear ideal for study as a dispersed phase in aluminum alloys. Furthermore, our previous studies of bonding, crystal structure, and phase stability in other intermetallics[10] give us confidence that such structural stability studies will work well for transition-metal (TM) trialuminides as well.

In this paper, we study (i) the structural stability and electronic structure of $ScAl_3$ and $ZrAl_3$ in two different crystal structures ($L1_2$ and $D0_{22}$) using the total-energy local-density-functional approach[11] as implemented in the all-electron, semirelativistic linear muffin-tin orbital (LMTO) method with the atomic-sphere approximation[12] and (ii) the stability of Sc stabilized cubic $ZrAl_3$. Computational details are presented in Sec. II, results for $ScAl_3$ and $ZrAl_3$ in Sec. III, and the possible stabilization of cubic $ZrAl_3$ by Sc addition is considered in Sec. IV.

II. COMPUTATIONAL DETAILS

The total-energy electronic band structure was obtained using the all-electron self-consistent linear muffin-tin orbital method associated with the atomic-sphere approximation. The Hedin and Lundqvist[13] and von Barth–Hedin[14] formalism for the exchange and correlation potential was adopted.

The total energies of $ScAl_3$ and $ZrAl_3$ were calculated as a function of the lattice constant [or equivalently the Wigner-Seitz radius (r_{WS})] using 60 k points within a $\frac{1}{48}$ (for the cubic $L1_2$ structure) and a $\frac{1}{16}$ (for the tetragonal $D0_{22}$ structure) irreducible wedge of the first Brillouin zone (IBZ). For the tetragonal $D0_{22}$ case, the c/a ratio was taken as the average experimental value (2.20–2.24) for the stable $D0_{22}$ TM trialuminides and kept constant (=2.21 for $ScAl_3$ and 2.23 for $ZrAl_3$). In general, in the linear tetrahedron method, the total energy depends linearly on[15] $(n_k)^{-2/3}$, where n_k is the number of k points within an irreducible wedge of the Brillouin zone (IBZ). Thus, an accurate value of the total energy can be obtained by extrapolating the values of the total energy calculated with different numbers of k points to an infinite number of k points. However, our previous study of Ni_3V (Ref. 10) showed that 60 k points within the irreducible wedge of the BZ is good enough to determine the stable phase because the energy difference caused by structural factors is nearly 1 order of magnitude larger than that due to the finiteness of the number of k points used. Nevertheless, the extrapolated value of the total energy was adopted to calculate the formation energy, calculated as the energy difference between the compound and the weighted sum of the constituent metals [calculated by the same LMTO procedure to be −1524.9823 Ry per atom for (hcp) Sc, −7190.3745 Ry per atom for (hcp) Zr, and −483.8320 Ry per atom for (fcc) Al]. A parabolic fitting procedure was adopted to obtain the bulk modulus. Since its calculation requires the second derivative of the total energy, the calculated value of the bulk modulus involves some numerical uncertainty, which is typically about[15] 10–15%. For simplicity, we assumed that the transition metal and the aluminum atoms have the same size Wigner-Seitz radius.

III. RESULTS FOR $ScAl_3$ AND $ZrAl_3$

As mentioned above, since most of the early transition-metal trialuminides have the $D0_{22}$ structure, we studied the structural stability of $L1_2$ versus $D0_{22}$ for $ScAl_3$ and $ZrAl_3$. Figure 2 exhibits the total energy as a function of the Wigner-Seitz sphere radius (r_{WS}) for $ScAl_3$ in these two different structures. It is seen clearly that $ScAl_3$ in the $L1_2$ structure is energetically favored compared to the $D0_{22}$ structure; in the entire region shown, the total energy of the $L1_2$ structure is about 0.4–0.5 eV per formula unit lower than that of the $D0_{22}$ structure. The calculated cohesive properties [including the equilibrium Wigner-Seitz radius (r^0_{WS}), lattice constants (a and c), bulk modulus, and formation energy] are listed in Table II. The calculated lattice constant (4.055 Å) for cubic ($L1_2$) $ScAl_3$ is in good agreement with the experimental value[4] (4.10 Å).

The total energy for both the $L1_2$ and $D0_{22}$ phases of $ZrAl_3$ was calculated as a function of the Wigner-Seitz sphere radius (cf. Fig. 3). The total energy for the cubic $L1_2$ phase of $ZrAl_3$ is only slightly higher (about 0.07 eV per formula unit) than that for the $D0_{22}$. This result indicates that it is energetically favorable for $ZrAl_3$ to have an antiphase boundary in the two neighboring cubic $L1_2$

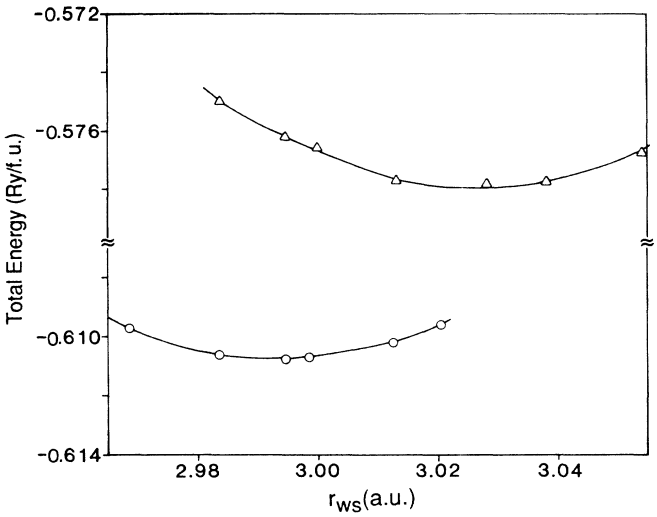

FIG. 2. Total energy [from which −2976 Ry/(formula unit) has been subtracted] as a function of the Wigner-Seitz radius and its structural dependence for $ScAl_3$, using 60 k points within the IBZ: circles and triangles denote the $L1_2$ and the $D0_{22}$ structures, respectively.

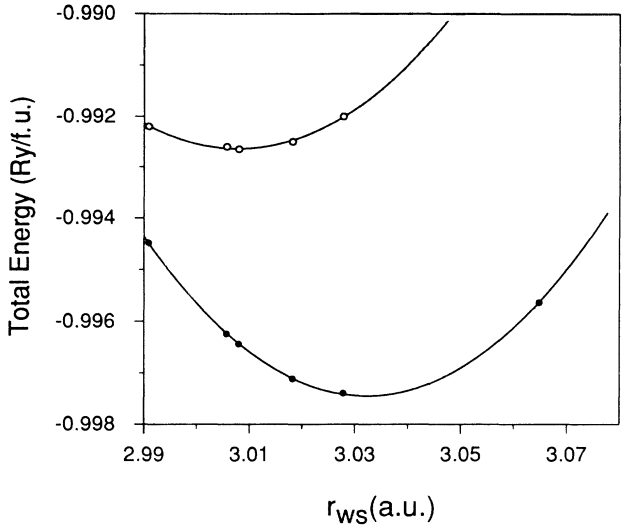

FIG. 3. Total energy [from which −8641 Ry/(formula unit) has been subtracted] as a function of the Wigner-Seitz radius and its structural dependence for $ZrAl_3$ using 60 k points with the IBZ: open and solid circles denote the $L1_2$ and the $D0_{22}$ structures, respectively.

unit cells. In fact, the stable $D0_{23}$ structure for $ZrAl_3$ has two antiphase boundaries in every four adjacent cubic $L1_2$ unit cells of $ZrAl_3$ (cf. Fig. 1). For comparison with the results obtained for $ScAl_3$, the calculated cohesive properties for $ZrAl_3$ are also listed in Table II. The calculated lattice constant (4.073 Å) for $ZrAl_3$ in the $L1_2$ structure is in excellent agreement with experiment (4.0731 Å).[3] The bulk modulus (1.0 Mbar) appears to be consistent with the observed Young's modulus (196 GPa) (Ref. 16) from the following argument. Now, the bulk modulus is related to the Young's modulus via the Poisson ratio σ [$B = Y/3(1-2\sigma)$]. Assuming $\sigma = 0.23$ (the experimental value for $NbAl_3$),[17] the Young's modulus will be ~150 GPa.

While no experimental data on the heat of formation are available for metastable cubic $ZrAl_3$ to our knowledge, it is interesting that the calculated formation energy (40.0 kcal/mole) for the $L1_2$ phase is comparable with the experimental values of the heat of formation for $TiAl_3$ [35.3 ± 1.2 (Ref. 18) and 34.0 (Ref. 19) kcal/mole] and for $ZrAl_2$ (40.8 kcal/mole) (Ref. 20) in the hexagonal ($C14$) phase.

To understand the phase stability of $ScAl_3$ and $ZrAl_3$, we inspect the electronic structures of the cubic $ScAl_3$ and $ZrAl_3$ in terms of the bonding character between the transition metal (Sc or Zr) and aluminum. As a first crude approximation, the overall electronic structure of the transition-metal trialuminides can be viewed simply as arising from a superposition of the free-electron-like background (mainly attributed to the Al s and Al p bands) and the transition-metal (Sc or Zr) d bands with several "extra" features arising mainly from the (Sc or Zr) d-(Al) p hybridization. As seen in the density of states (DOS) plots given in Figs. 4(a) and 5(a), the occupied bandwidth of Sc (or Zr) in the Sc (or Zr) aluminum-rich compounds is significantly wider (~4 eV) than that

TABLE II. Equilibrium lattice constants a and c, Wigner-Seitz radii r_{WS}^0, bulk moduli B, and formation energies ΔE for $ScAl_3$ and $ZrAl_3$ in the $L1_2$ and $D0_{22}$ structures.

Compounds		a (Å) calc.	a (Å) expt.	c (Å) calc.	c (Å) expt.	r_{WS}^0 (a.u.)	B (Mbar)	ΔE (kcal/mole)
$ScAl_3$	$L1_2$	4.055	4.10[a]			2.995	0.93	43.0
	$D0_{22}$	3.966		8.765		3.028	0.90	33.3
$ZrAl_3$	$L1_2$	4.073	4.0731[b]			3.008	1.0	40.0
	$D0_{22}$	3.954		8.817		3.028		~41
	$D0_{23}$		4.013[c]		17.32[c]	3.040		

[a] Reference 4.
[b] Reference 3.
[c] Reference 19.

in pure hcp Sc (or Zr) metal, respectively. Since the bandwidth reflects the degree of orbital overlap, a characteristic feature for the transition-metal trialuminides (such as $ScAl_3$ and $ZrAl_3$) is that there is a strong hybridization between transition-metal d and Al p states. As a result of forming the bonding and antibonding states, the entire band can be roughly divided into three regions separated by the two deep valleys (or pseudogaps)[21] located at about 0.4 eV for $ScAl_3$ (-0.5 eV for $ZrAl_3$) [cf. Figs. 4(b) and 5(b)] and 5–6 eV, respectively. The strongly hybridized Zr (or Sc) d and Al p bonding states are located in the entire region between -0.9 eV and the Fermi level for $ScAl_3$ (-0.5 eV for $ZrAl_3$), and the antibonding states are located in the region above 5–6 eV. Be-

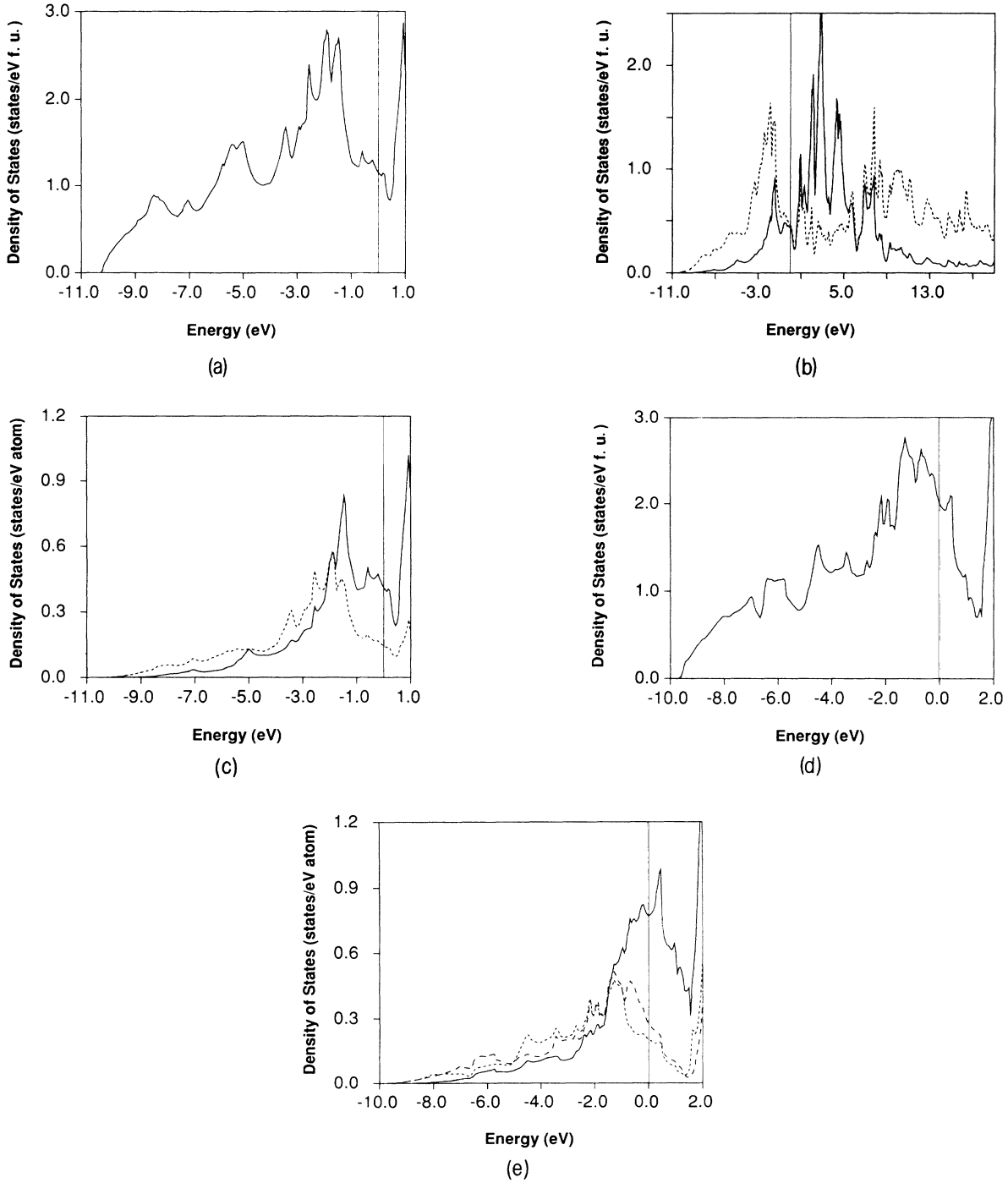

FIG. 4. Total and partial density of states for $ScAl_3$ in the $L1_2$ [(a), (b), and (c)] and the DO_{22} [(d) and (e)] structures; in (b) and (c), solid and dashed lines denote Sc 3d and Al 3p states, respectively; in (e) solid, short-dashed, and long-dashed lines denote Sc 3d, Al(1) 3p, and Al(2) 3p states, respectively. Al(1) denotes aluminum atoms located in the same (001) plane as Sc, and Al(2) denotes atoms located in (001) planes below or above the Sc layer.

tween the bonding and the antibonding states there are Zr (or Sc) nonbonding states which still contain significant Al p states.

As we demonstrated previously for other aluminides,[22] the essential contribution to the cohesion (i.e., stability) of the transition-metal trialuminides is maximizing the filling of bonding states. For the most stable structure, there is enough room to accommodate all its valence electrons into the bonding states so as to bring the Fermi level to a valley position separating bonding and nonbonding (or antibonding) states; in other words, the stable structure is often characterized by a low[10,22] $N(E_F)$. Indeed the cubic $ScAl_3$ phase has an extremely low $N(E_F)$ value (1.16 states/eV formula unit) (cf. Table III)

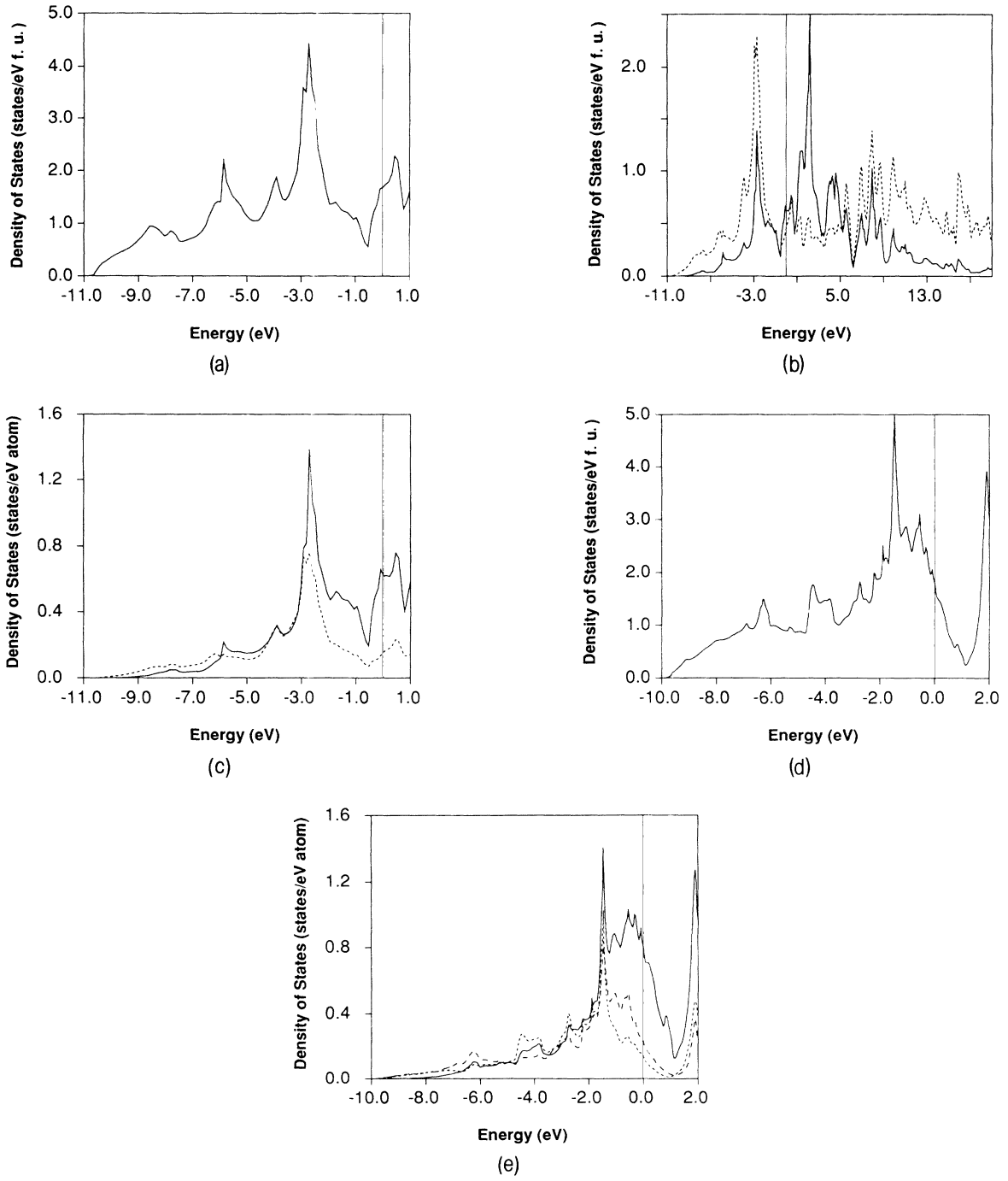

FIG. 5. Total and partial density of states for $ZrAl_3$ in the $L1_2$ [(a), (b), and (c)] and the $D0_{22}$ [(d) and (e)] structures; in (b) and (c) solid and dashed lines denote Zr 4d and Al 3p states, respectively; in (e) solid, short-dashed, and long-dashed lines denote Zr 4d, Al(1) 3p, and Al(2) 3p states, respectively. Al(1) denotes aluminum atoms located in (001) plane at the same layer as Zr, and Al(2) located in (001) planes below or above the Zr layer.

TABLE III. Total and partial density of states (projected by angular momentum and atom) at E_F in (states/eV formula unit) for $ScAl_3$ and $ZrAl_3$ in the $L1_2$ and $D0_{22}$ structures.

MAl_3		D_s^M	D_p^M	D_d^M	D_s^{Al}	D_p^{Al}	D_d^{Al}	D_{tot}
$ScAl_3$	$L1_2$	0.01	0.03	0.42	0.04	0.44	0.22	1.16
	$D0_{22}$	0.02	0.06	0.76	0.08	0.75	0.31	1.98
$ZrAl_3$	$L1_2$	0.04	0.03	0.59	0.08	0.41	0.39	1.55
	$D0_{22}$	0.01	0.04	0.81	0.04	0.58	0.32	1.80

because 12.5 electrons per formula unit (cf. Table IV) can be accommodated in the bonding region. As a result, all 12 electrons per formula unit for the cubic $ScAl_3$ nearly fill up the bonding states; this increases the bond strength and brings E_F close to the valley separating the bonding and nonbonding states [Figs. 4(a) and 4(c)]. By contrast, for the tetragonal $D0_{22}$ phase E_F is still located in the Sc d and Al p bonding region [cf. Figs. 4(d) and 4(e)], but it now lies just on a peak of the Sc d partial density of states (1.98 states/ev formula unit) and results in a higher density of states at E_F than cubic $ScAl_3$, which was characterized by an extremely low $N(E_F)$ value. In particular, we note that the occupied portion (or band filling) of the bonding states for the cubic $L1_2$ phase is obviously larger than that for the tetragonal phase; hence, for $ScAl_3$ the cubic phase will be a strongly bonded phase as compared to the tetragonal $D0_{22}$ phase. (We will discuss this feature in more detail in Sec. IV.)

On the other hand, for cubic $ZrAl_3$, an additional 0.64 electrons per formula unit (cf. Table IV) fill states above the valley into the nonbonding region. As a result, the position of E_F for cubic $ZrAl_3$ lies on the shoulder (a small peak) in the total (partial) density of states [Figs. 5(a) and 5(c)] instead of in the valley for cubic $ScAl_3$ and thus may cause cubic $ZrAl_3$ to be a metastable phase with respect to the tetragonal $D0_{23}$ phase. As proposed by Gelatt *et al.*,[23] the phase stability is dominated by two ingredients: (i) the strong hybridization between the transition-metal d states and the aluminum p states, and (ii) the weakening of the bonding between the transition-metal atoms (i.e., nonbonding states in the trialuminides) caused by the increased transition-metal atom separation which results from inserting the aluminum atoms. For $ZrAl_3$ in the nonbonding region the second factor dominates over the first, and therefore, filling the nonbonding hybrids reduces its relative stability.[24] Alternatively, since for the $D0_{22}$ phase of $ZrAl_3$ the bonding states can accommodate a total of 14 valence electrons (cf., Table IV), its 13 valence electrons can be completely placed into the bonding region [cf. Figs. 5(d) and 5(e)] leading to a slightly higher stability with respect to the cubic phase. In addition, it is interesting to note that the tetragonal $D0_{22}$ phase has a relatively higher stability on going from $ScAl_3$ to $ZrAl_3$, which can be simply understood in the rigid band sense in terms of filling the bonding states.

TABLE IV. The width of the occupied states (W_{occ}), of the bonding states (W_b), W_{occ}/W_b, and the number of the valence electrons to be accommodated in the bonding states (n_b) for $ScAl_3$, $ZrAl_3$, and $(Zr_{0.5}Sc_{0.5})Al_3$ (width in eV, n_b in electrons).

		W_{occ}	W_b	W_{occ}/W_b	n_b
$ScAl_3$	$L1_2$	10.26	11.70	0.96	12.45
	$D0_{22}$	9.69	11.07	0.87	13.96
$ZrAl_3$	$L1_2$	10.71	10.21	1.05	12.36
	$D0_{22}$	9.69	10.80	0.90	14.0
$(Zr_{0.5}Sc_{0.5})Al_3$		10.50	10.37	1.01	12.39

In summary, the correlation between the structural stability and the filling of the bonding states for the two ($L1_2$ and $D0_{22}$) structures in $ScAl_3$ and $ZrAl_3$ is shown in Table IV. Here we denote the width of the occupied states by W_{occ} and the width of the bonding states W_b as the distance from the bottom of the band to E_F and to the valley, respectively. The ratio W_{occ}/W_b is used to evaluate the occupied portion of the bonding states, i.e., the band filling of the bonding states. We can clearly see from Table IV that the stable phase for a given compound is always the one having the maximum filling of the bonding states.[25]

IV. Sc STABILIZATION OF CUBIC $ZrAl_3$ PRECIPITATES

Based on the argument of the correlation between the stability and the filling of the bonding states (equivalently, the low density of states at E_F), we expect that the cubic trialuminides $Zr_{1-x}Sc_xAl_3$ and $Ti_{1-x}Sc_xAl_3$ ($x > 0.55$) might have a low $N(E_F)$ in the rigid band sense, because the valence electrons which occupy nonbonding states in the cubic $ZrAl_3$ will be removed when Sc is added to $ZrAl_3$. From these arguments it appears that Sc may be used to stabilize the metastable cubic $ZrAl_3$ phase.

For these reasons, we have investigated the structural stability of the hypothetical cubic trialuminide $(Zr_{0.5}Sc_{0.5})Al_3$ relative to $ScAl_3$ and $ZrAl_3$. We assumed $(Zr_{0.5}Sc_{0.5})Al_3$ has a double fcc-like cubic cell containing two formula units and that half of the Zr sites in $ZrAl_3$ are occupied by Sc atoms, i.e., Zr occupies the top and the bottom corner sites, and Sc the middle corner sites, or vice versa (cf. Fig. 6). As a result, we can discriminate three different kinds of aluminum atoms according to their atomic environment: Al(1) and Al(3) represent aluminum atoms in a (001) plane with the same layer as Zr (Sc) atoms, and Al(2) are the Al atoms sitting in a

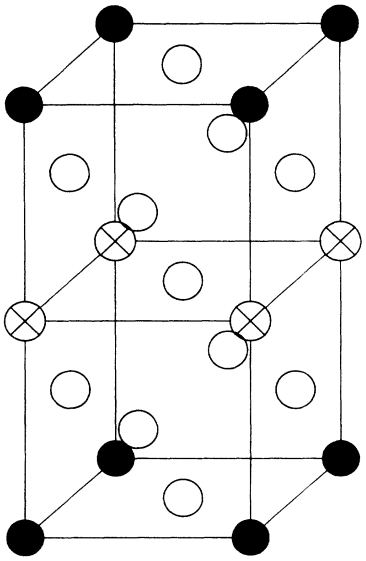

FIG. 6. The unit cell of the hypothetical trialuminide $(Zr_{0.5}Sc_{0.5})Al_3$. Solid, crossed, and open circles denote Zr, Sc, and Al atoms, respectively. Al(1) and Al(3) denote aluminum atoms located in the same (001) plane as Zr and Sc atoms, respectively, and Al(2) denotes atoms located in the (001) plane below or above the Zr (or Sc) layer.

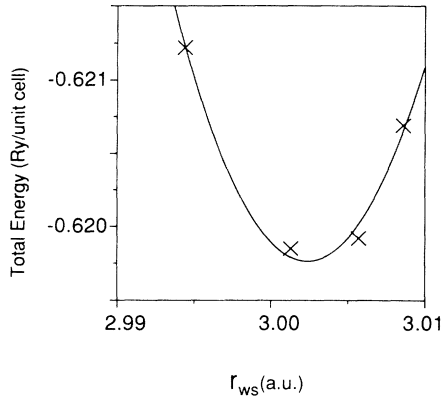

FIG. 7. Total energy [from which −11 618 Ry(unit cell) has been subtracted] as function of the Wigner-Seitz sphere radius r_{WS} for $(Zr_{0.5}Sc_{0.5})Al_3$ (cf. Fig. 6) using 60 k points within the IBZ.

(001) plane below or above the Zr (or Sc) layer. The dependence of the total energy versus Wigner-Seitz radius for $(Zr_{0.5}Sc_{0.5})Al_3$ is shown in Fig. 7. Note that after extrapolating to an infinite number of k points the equilibrium total energy for $(Zr_{0.5}Sc_{0.5})Al_3$ is indeed lower [by about 18–19 mRy (i.e., ~0.24 eV) per unit cell] than the sum of the total energies of the $ZrAl_3$ and the $ScAl_3$ compounds (cf. Table V). This result indicates that forming ordered cubic $(Zr_{0.5}Sc_{0.5})Al_3$ by adding Sc into cubic $ZrAl_3$ is energetically favored as compared with its constituents, $ScAl_3$ and $ZrAl_3$.

Moreover, it is interesting to note that the equilibrium lattice constant obtained from the minimum of the total energy has the same value (4.066 Å) (or equivalently $r_{WS}=3.003$ a.u.) as the average value of the lattice constants (4.064 Å) of $ScAl_3$ and $ZrAl_3$ within the precision of the calculation. This result may be taken to mean that the rigid band picture holds well for these transition-metal trialuminides (as will be further discussed when we consider the electronic structure.) For comparison, the equilibrium lattice constants, total energies, total density of states at the Fermi level, and values of E_A,E_B,E_C,E_D,E_F for the three trialuminides [$ScAl_3$, $(Zr_{0.5}Sc_{0.5})Al_3$, and $ZrAl_3$] are listed in Table V. Here, E_A, E_B, and E_C denote the energies corresponding to the three features (A, B, and C) below the Fermi level in the density of state curves [cf. Fig. 8(a)], and E_D represents the energy of the valley D, which separates the bonding and the nonbonding states in the DOS; all energies are measured from the bottom of the valence band.

In order to gain insight into the correlation between the structural stability for different compounds and its electronic structures, we compare the total DOS of $(Zr_{0.5}Sc_{0.5})Al_3$ [Fig. 8(a)] with that of cubic $ScAl_3$ [Fig. 4(a)] and cubic $ZrAl_3$ [Fig. 5(a)]. First of all, note that the overall features for these three transition-metal trialuminides resemble each other. For all three, there are three prominent features (denoted by A, B, and C) below the Fermi level, and a deep valley D. The positions and the widths of all three features for the different trialuminides are seen to coincide with each other, after the

TABLE V. Values of the equilibrium lattice constant, total energy (E_{tot}), density of states at E_F [$N(E_F)$], E_F, E_A, E_B, E_C, and E_D for the cubic trialuminides [$ScAl_3$, $(Zr_{0.5}Sc_{0.5})Al_3$, and $ZrAl_3$], where E_A, E_B, E_C, E_D, and E_F are measured from the bottom of the valence band (as defined in the text). E_{tot} obtained after extrapolating to an infinite number of k points within the IBZ. f.u. denotes formula unit.

	$ScAl_3$	$(Zr_{0.5}Sc_{0.5})Al_3$	$ZrAl_3$
a (Å)	4.055	4.067	4.073
E_{tot} [Ry/(unit cell)]	−2976.6156	−11 618.632	−8641.9991
$N(E_F)$ (states/eV f.u.)	1.55	1.10	1.16
E_A (eV)	1.9	2.0	2.1
E_B (eV)	4.9,5.3	4.8	4.8
E_C (eV)	8.4	7.9	8.0
E_D (eV)	10.7	10.4	10.1
E_F (eV)	10.27	10.50	10.69

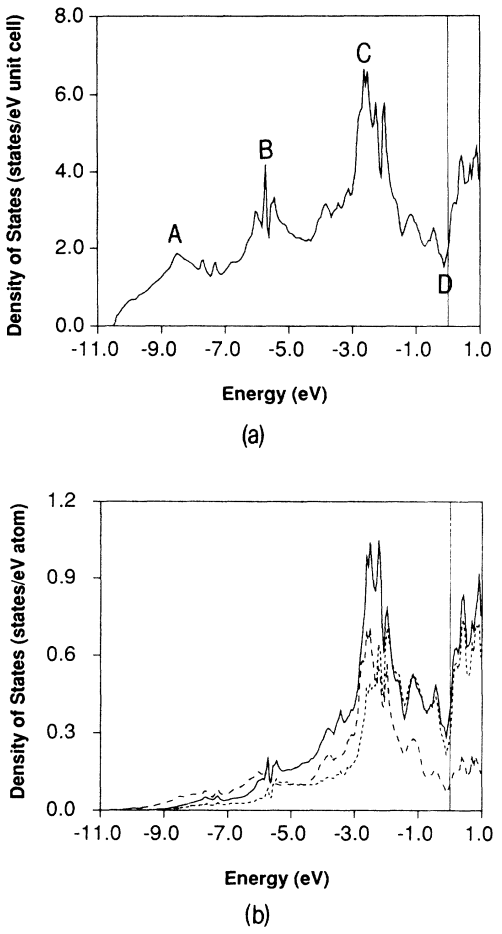

FIG. 8. (a) total and (b) partial density of states for $(Zr_{0.5}Sc_{0.5})Al_3$, where *A*, *B*, and *C* denote the three features below E_F, and *D* denotes the valley in the density of states curve. Solid, short-dashed, and long-dashed lines represent Zr 4*d*, Sc 3*d*, and Al(1) 3*p* states, respectively. Al(1) represents aluminum atoms located in the (001) plane at the same layer as Zr atoms (cf. Fig. 6).

bottom of their valence bands are shifted to coincide with each other. Only the position of feature *C* of $ScAl_3$ has been shifted (by about 0.5 eV) towards lower binding energy with respect to that of $(Zr_{0.5}Sc_{0.5})Al_3$. Since it has been known that this most prominent peak *C* represents strong hybridization between the transition-metal *d* and Al *p* states [cf. Fig. 8(b)], and dominates the cohesive properties in the transition-metal trialuminides, it partly contributes to the higher stability for $(Zr_{0.5}Sc_{0.5})Al_3$ as compared with its parent aluminide $ScAl_3$.

As previously discussed, the main contribution to the cohesion (or stability) of the trialuminides can be understood in terms of the band filling of its bonding states. Note that the bonding states region denoted by energy E_D in the DOS becomes narrower upon going from $ScAl_3$ (10.7 eV) to $(Zr_{0.5}Sc_{0.5})Al_3$ (10.3 eV) and to $ZrAl_3$ (10.1 eV). The bonding region E_D is higher than E_F for $ScAl_3$; all 12 electrons occupy the bonding states of $ScAl_3$. On the other hand, since E_D is located below E_F in $ZrAl_3$, part of the valence electrons fill states (above the pseudogap) which are nonbonding and this may cause cubic $ZrAl_3$ to be a metastable phase. However, for $(Zr_{0.5}Sc_{0.5})Al_3$, the closeness between E_D and E_F means that a maximum number of bonding states are occupied (cf. Table IV). Therefore, according to the diatomic bonding arguments suggested by Gelatt *et al.*,[23] filling bonding states increases the bond strength, and the cubic trialuminide $(Zr_{0.5}Sc_{0.5})Al_3$ will be more favored energetically as compared with $ScAl_3$ itself and also with the mixture of $ScAl_3$ and $ZrAl_3$. In fact, our calculated total energy for $(ZrSc)Al_3$ is indeed 0.24 eV per unit cell lower than the sum of the total energies of $ScAl_3$ and $ZrAl_3$ (cf. Table V). Further, the portion of the occupied valence band defined as the distance between the bottom of the valence band and E_F widens with increasing number of valence electrons upon going from $ScAl_3$ (10.27 eV) to $(Zr_{0.5}Sc_{0.5})Al_3$ (10.50 eV) to $ZrAl_3$ (10.69 eV) (cf. Table V). Surprisingly, the average occupied bandwidth of $ZrAl_3$ and $ScAl_3$ (10.49 eV) again agrees quite well with the calculated occupied bandwidth of $(Zr_{0.5}Sc_{0.5})Al_3$ (10.50 eV) within the error of the calculation. The additional valence electrons of $ZrAl_3$ may indeed be considered to be simply added into the unoccupied bonding states of the $ScAl_3$ in the rigid band sense, when Zr is added into $ScAl_3$. Finally, a notable feature is that among these three transition-metal trialuminides, $(Zr_{0.5}Sc_{0.5})Al_3$ has the lowest density of states at the Fermi level (1.10 states/eV formula unit) (cf. Table V); again, the energetically favored compound leads to a low $N(E_F)$ in the aluminides.

In conclusion, we have demonstrated that the Sc additions in $ZrAl_3$ appear to be a good way to stabilize for its metastable cubic phase and hence that cubic $Zr_{1-x}Sc_xAl_3$ (or possibly $Ti_{1-x}Sc_xAl_3$) may be a good candidate as a dispersed phase in the aluminum alloys for elevated temperature applications.

ACKNOWLEDGMENTS

This work was supported by the Air Force Office of Scientific Research, Grant No. 88-0346, and by a grant of computing time at the Wright-Patterson AFB Supercomputing Center. Discussions with D. Dimiduk are gratefully acknowledged. We thank M. E. Fine for discussions of precipitates in aluminum alloys and T. Hong for helpful collaboration and discussions.

[1]W. B. Pearson, *A Handbook of Lattice Spacings and Structures of Metals and Alloys* (Pergamon, Oxford, 1967), Vol. 2.

[2]*Structure Reports,* edited by W. B. Pearson (International Union of Crystallography, Utrecht, 1967), Vol. 32A, p. 14.

[3]T. Ohashi and R. Ichikawa, Metall. Trans. **3**, 2300 (1972).

[4]V. W. Rechkin, L. K. Lamikhov, and T. I. Samsonova, Kristallografiya **9**, 405 (1964) [Sov. Phys.— Crystallog. **9**, 325 (1964)].

[5]*Binary Alloy Phase Diagrams,* edited by T. B. Massalski (American Society for Metals, Metal Park, Ohio, 1986), Vol 1.
[6]E. J. Kubel, Adv. Mater. Proc. Metal Prog. **130**, 43 (1986).
[7]M. E. Fine, Metall. Trans. A **6**, 625 (1975).
[8]S. Tsunekawa and M. E. Fine, Scripta Metall. **16**, 391 (1982); M. Zedalis and M. E. Fine, Scripta Metall. **17**, 1247 (1983).
[9]Y. C. Chen, M. E. Fine, J. R. Weertman, and R. E. Lewis, Scripta Metall. **21**, 1003 (1987).
[10]J.-H. Xu, T. Oguchi, and A. J. Freeman, Phys. Rev. B **35**, 6940 (1987).
[11]W. Kohn and L. J. Sham, Phys. Rev. **140**, A1133 (1965).
[12]O. K. Andersen, Phys. Rev. B **12**, 3036 (1975).
[13]L. Hedin and B. Lundqvist, J. Phys. C **4**, 2064 (1971).
[14]U. von Barth and L. Hedin, J. Phys. C **5**, 1629 (1972).
[15]H. J. F. Jansen and A. J. Freeman, Phys. Rev. B **30**, 561 (1984).
[16]M. S. Zedalis, M. V. Ghate, and M. E. Fine, Scripta Metall. **19**, 647 (1985).
[17]J. H. Schneibel, P. F. Becher, and J. A. Morton, J. Mater. Res. **3**, 1272 (1988).
[18]O. Kubaschewski, E. L. Evans, and C. B. Alcock, *Metallurgical Thermochemistry, 4th ed.* (Pergamon, Oxford, 1967).
[19]*Smithells Metals Reference Book, 6th ed.,* edited by E. A. Brandes (Butterworths, London, 1983).
[20]A. Schneider, H. Klotz, J. Stendel, and G. Strauss, Pure Appl. Chem. **2**, 13 (1961).
[21]A. Pasturel, C. Colinet, and P. Hicter, Physica B+C (Amsterdam) **132**, 177 (1985).
[22]J.-H. Xu and A. J. Freeman, Phys. Rev. B **40**, 11 927 (1989).
[23]C. D. Gelatt, A. R. Williams, and V. L. Moruzzi, Phys. Rev. B **27**, 2005 (1983).
[24]C. Colinet, A. Pasturel, and K. H. J. Bushow, Physica B (Amsterdam) **150**, 397 (1988).
[25]R. Hoffmann, Rev. Mod. Phys. **60**, 601 (1982).